PCCP

Chemical bonding analysis of excited states using the Adaptive Natural Density Partitioning method

Journal:	*Physical Chemistry Chemical Physics*
Manuscript ID	CP-ART-01-2019-000379.R1
Article Type:	Paper
Date Submitted by the Author:	27-Mar-2019
Complete List of Authors:	Tkachenko, Nikolay; Utah State University, Department of Chemistry and Biochemistry Boldyrev, Alexander; Utah State University, Department of Chemistry and Biochemistry

Chemical bonding analysis of excited states using the Adaptive Natural Density Partitioning method

Nikolay V. Tkachenko and *Alexander I. Boldyrev**

Department of Chemistry and Biochemistry, Utah State University, Logan, Utah 84322, United States

** Corresponding author, e-mail: a.i.boldyrev@usu.edu*

ABSTRACT: A novel approach to chemical bond analysis for excited states has been developed. Using an extended adaptive natural density partitioning method (AdNDP) as implemented in AdNDP 2.0 code, we obtained chemically intuitive bonding patterns for the excited states of H_2O, B_5^+, and $C_2H_4^+$ molecules. The deformation pathway in the excited states could be easily predicted based on the analysis of the chemical bond pattern. We expect that this new method of chemical bonding analysis would be very helpful for photochemistry, photoelectron spectroscopy, electron spectroscopy and other chemical applications that involved excited states.

KEYWORDS: chemical bonding, excited states, chemical bonding in excited molecules, AdNDP 2.0

INTRODUCTION

The theoretical study of excited states is an important, developing part of modern physical chemistry. Due to the intensive development of computational methods, more and more accurate tools for analyzing excited molecules appear in the hands of chemists. Various predictive models are widely used in modern photochemistry and spectrometry. However, there are still very few methods to analyze chemical bonding of the excited state using basic chemical concepts.

The theory of chemical bonding is still an ambiguous area of physical chemistry. Before the formulation of quantum mechanics, Lewis proposed the most generally accepted theory of chemical bonding [1]. His empirical model emphasized the key idea that the electron pair is the main element of a chemical bond, becoming an essential part of modern "chemistry language". However, during the development of quantum mechanics, new approaches were proposed. In 1931, Hund [2] and in 1932 Mulliken [3] introduced a theory of molecular orbitals (MO) which provided a new delocalized way of describing electrons in the chemical system. Chemical bonding theory based on the alternative to MO way was proposed by Pauling [4,5], Heitler, London [6] and Slater [7,8]. They introduced a valence bond theory which was built on the concept of hybrid orbitals and perfectly predicts the chemical bond of the first two rows of the periodic table.

A great contribution to the description of chemical systems and chemical bonding was made by methods that do not directly reveal the concept of chemical bond. Those methods are based on the various forms of electron density distribution analysis [9-24]. One example of these methods includes a quantum theory of atoms in molecules (QTAIM) [9] that is based on the topology of the electron density. Another example is an electron localization function (ELF) [16] that is based on the local quantum-mechanical function, related to the Pauli exclusion principle. Bonds in a chemical system can also be defined using various bond indexes. The general definition

of the bond index was given by Wiberg [25]. Since then, a plenty of different bond indices were proposed for describing chemical bonding patterns [26-37].

Electron density localization methods based on the invariance of the wave function with respect to the unitary transformation are successfully used to obtain an exhaustive chemical bonding interpretation of ground state systems. In the second half of 20th century, a variety of localization methods were proposed [38-43]. The extraction of localized bonding pattern from an electron-density function served as a bridge linking two paradigms (quantum chemistry and classical approaches) that are completely distinct from each other.

The applicability of some aforementioned methods can be extended for use for electronic excited states. The technique associated with the analysis of molecular orbitals is the most widely used since a lot of computational methods have been developed to accurately predict an electronic structure of excited state compounds [44]. Several approaches based on localization functions has also been proposed [45, 46]. Thus, introduced by Burnus and coworkers time-dependent ELF [46] provides a visual understanding of the dynamics of excited electrons. However, those approaches are limited since molecular orbitals are not well defined in the excited states due to the multiconfigurational nature of the wave function. Recently proposed computational methods that can describe molecular orbitals of electronic excited states are not widely available [47, 48]. Another way to analyze excited states is Interacting Quantum Atoms (IQA) method [49] based on the QTAIM. That method was successfully applied to describe basic reaction mechanisms including excitation processes as well as bonding in excited states of small molecules [50-53]. Likewise, a new tool (the density overlap region indicator) for visualizing interactions in the excited states was proposed [54]. That method depends only on electron density and its derivatives, which can bypass restrictions associated with multiconfigurational wave function.

Previously, we introduced the Adaptive Natural Density Partitioning algorithm [55,56] (AdNDP), a powerful approach for the analysis of electron density function. This method allows us to obtain a compact, intuitively simple description of the chemical bonding in molecules with a non-classical bonding pattern. Due to the extension of the Lewis description, AdNDP is a good implementation to search for delocalized *n*-center 2 electron bonds (n>2). In the course of our work, we expanded the applicability of the AdNDP method and proposed an approach for studying chemical bonds in the excited state to predict the deformation of the structure under vertical excitation.

COMPUTATIONAL METHODS

For the geometry optimization and electron-density calculations, CASSCF method [57] was used. For each molecule different size of an active space as well as different basis set were chosen (CASSCF(8,10)/aug-cc-pvtz [58] for H_2O, CASSCF(14,10)/6-311G** [59] for B_5^+ and CSSSCF(7,9)/aug-cc-pvdz for $C_2H_4^+$). Excited state calculations were performed at the same level of theory using the second root of the CASSCF calculations, thus the first singlet (or doublet in case of $C_2H_4^+$) excited state was studied for each molecule. To check the vibrational structure and calculate an energy barrier of the rotation along the C-C bond for $C_2H_4^+$ species, CCSD(T)/cc-pvqz [61, 62] level of theory was used. Chemical bonding analysis was performed via extended adaptive natural density partitioning algorithm as implemented in AdNDP 2.0 code. The new version was written using Python3.7 programming language.

From a computational point of view, the main bond search algorithm remains the same in AdNDP 2.0 as in the original AdNDP code. In the current version of the AdNDP we are partitioning one-electron density matrix. In the initial designing of the AdNDP method, we followed general ideas of the NBO analysis proposed by Weinhold [43]. The complete description

of the AdNDP algorithm can be found elsewhere [56]. Nonetheless, for a better understanding of the new features of the AdNDP algorithm, we need to introduce some terms and definitions. We will call $\gamma(\bar{r}_1 \,|\, \bar{r}_1')$ the spinless first-order reduced density operator:

$$\gamma(\bar{r}_1 \,|\, \bar{r}_1') = N \int \psi(\bar{r}_1,\bar{r}_2,...,\bar{r}_N)\psi^*(\bar{r}_1',\bar{r}_2,...,\bar{r}_N)d^3\bar{r}_2...d^3\bar{r}_N \quad \text{(I)}$$

Where ψ is any N-electron wave function, $\bar{r}_1,\bar{r}_1',\bar{r}_2,...,\bar{r}_N$ are generalized coordinates of i^{th} electron. For any complete orthonormal basis set of atomic orbitals $\{\chi_k\}$, the spinless first-order reduced density operator can be expanded as:

$$\gamma(\bar{r}_1 \,|\, \bar{r}_1') = \sum_{k,l} P_{kl}\chi_k(\bar{r}_1)\chi_l^*(\bar{r}_1') \quad \text{(II)}$$

The coefficients P_{kl} are elements of the density matrix $\boldsymbol{P}$ defined as:

$$P_{kl} = \int \chi_k^*(\bar{r}_1)\gamma(\bar{r}_1 \,|\, \bar{r}_1')\chi_l(\bar{r}_1')d^3\bar{r}_1 d^3\bar{r}_1' \quad \text{(III)}$$

Each diagonal matrix element P_{kk} corresponds to the occupation number (ON) of the k^{th} orbital function in the basis set $\{\chi_k\}$. Density matrix $\boldsymbol{P}$ can be represented in in the block form (IV) by splitting a basis $\{\chi_k\}$ into subsets of functions associated with a particular atomic center.

$$\boldsymbol{P} = \begin{bmatrix} \boldsymbol{P}_{11} & \cdots & \boldsymbol{P}_{1N} \\ \vdots & \ddots & \vdots \\ \boldsymbol{P}_{N1} & \cdots & \boldsymbol{P}_{NN} \end{bmatrix} \quad \text{(IV)}$$

Where $\boldsymbol{P}_{ij}$ is a submatrix of $\boldsymbol{P}$ and indices i,j correspond to the i^{th} and the j^{th} atomic center. By solving eigenproblem (V) for sub-blocks $\boldsymbol{P}^{(i_1,i_2,...,i_n)}$ of block matrix $\boldsymbol{P}$ we can obtain eigenvectors $v^{(i_1,i_2,...,i_n)}$ and eigenvalues $\lambda^{(i_1,i_2,...,i_n)}$ that describe particular bonding interaction between chosen atomic centers $i_1,i_2,...,i_n$.

$$\boldsymbol{P}^{(i_1,i_2,...,i_n)}v^{(i_1,i_2,...,i_n)} = \lambda^{(i_1,i_2,...,i_n)}\boldsymbol{S}^{(i_1,i_2,...,i_n)}v^{(i_1,i_2,...,i_n)} \quad \text{(V)}$$

Here and below we will call the square matrix $\boldsymbol{P}^{(i_1,i_2,\ldots,i_n)}$ composed of n sub-blocks of $i_1{}^{th}$, $i_2{}^{th}$, ... , $i_n{}^{th}$ centers as n-center sub-block matrix. An example of *3*-center sub-block matrix for atomic centers i_1, i_2, i_3 is shown below:

$$\boldsymbol{P}^{(ijk)} = \begin{bmatrix} \boldsymbol{P}_{i_1 i_1} & \boldsymbol{P}_{i_1 i_2} & \boldsymbol{P}_{i_1 i_3} \\ \boldsymbol{P}_{i_2 i_1} & \boldsymbol{P}_{i_2 i_2} & \boldsymbol{P}_{i_2 i_3} \\ \boldsymbol{P}_{i_3 i_1} & \boldsymbol{P}_{i_3 i_2} & \boldsymbol{P}_{i_3 i_3} \end{bmatrix} \quad \text{(VI)}$$

The search for bonds occurs sequentially starting from one-center elements (lone pairs) and ending at n-center bonds. Bonding elements found by the algorithm are checked for satisfaction of the condition $\lambda^{(i_1,i_2,\ldots,i_n)} \geq 2 - t_n$, where t_n is a threshold value that is set individually for each n. It is necessary to deplete density matrix $\boldsymbol{P}$ from the density associated with found bonds. Equation (VII) demonstrates the depletion process implemented in the AdNDP algorithm.

$$\tilde{\boldsymbol{P}} = \boldsymbol{P} - \lambda^{(i_1,i_2,\ldots,i_n)} \boldsymbol{v}^{(i_1,i_2,\ldots,i_n)} \boldsymbol{v}^{(i_1,i_2,\ldots,i_n)T} \quad \text{(VII)}$$

Where $\tilde{\boldsymbol{P}}$ is the depleted density matrix. The main improvements of the AdNDP 2.0 algorithm are listed below.

Distance restrictions

For the multi-center bond analysis, the original AdNDP algorithm investigates all possible n-center combinations in a molecule. For instance, for searching 6c-2e delocalized bonds in anthracene ($C_{14}H_{10}$) one needs to find eigenvalues and eigenvectors for 1.3×10^5 *6*-center sub-block matrices. However, from a chemical point of view, we know that most of those 6-atoms combinations are meaningless. In order to increase computational efficiency of the method, we decided to introduce distance restriction parameters in the AdNDP analysis. Initially, a list of all possible n-atoms combinations is created. After that, the algorithm reads the distance matrix of the system and checks each pair of atoms in each combination from the list, so that the distance between them is less than the given restriction parameter. Thus, the most distant atoms in each combination must

be closer than the restriction value. This restriction can be defined as follows: a set of atoms is taken into consideration only if all elements of the set lie in the intersection of all spheres of radius *R* centered on the atoms of the selected fragment, where *R* is distance restriction parameter that selected by the researcher. Described restriction parameters significantly reduce the number of considered sub-block matrices. Thus, for the anthracene we can reduce the number of analyzed *6*-center sub-block matrices from 1.3×10^5 to three by setting a 3Å limit. Thereby, the new feature of the algorithm noticeably reduces computational time.

Symmetric direct search

However, even with distance restriction parameters, one could face difficulties with obtaining a reasonable bonding pattern. For obscure cases, the density matrix could be analyzed by the "direct search" procedure, which allows searching multicentered bonds on given atomic centers. When specifying a fragment with the $i_1^{th}, i_2^{th},\ldots,i_n^{th}$ atomic centers, the eigenproblem is solved only for chosen *n*-center subblock matrices. The found eigenvector corresponding to the maximum eigenvalue are assigned to the nc-2e bond. Also, more than one fragment could be chosen at once. In this case the symmetry of the bonding picture preserves, since the search is conducted simultaneously on all the fragments. The densities associated with the found bonds are then subtracted from the full density matrix via equation (VII).

Bonding analysis of unrestricted and open shell systems

For the bonding analysis of an unrestricted case, two different density matrices in the natural atomic orbitals (NAO) basis set (for alpha and beta electrons) should be calculated. The maximum occupancy number that can be obtained for those matrices is 1.0 |e|. The AdNDP 2.0 code allows us to conduct a separate analysis of alpha and beta electron density matrices. In this case the

bonding pattern could be presented in terms of nc-1e bonds. Thus, the analysis for open shell systems or multiplet spin excited states now can be done via ADNDP 2.0 code.

Excited states bonding analysis

Analysis of the excited state electron density matrix in NAO basis set was implemented in the AdNDP 2.0 code. The density matrix should be calculated with CASSCF, since the feature is currently compatible only with this method. In the course of our work we used the second root of the CASSCF calculations, thus the density matrix of the first excited state is obtained. However, electron density for higher excited states can be analyzed. By using the flexibility of the AdNDP 2.0 method as well as new features of the algorithm one could easily obtains a bonding pattern for the excited states of the molecule and predicts subsequent geometric transformations occurring due to vertical excitation of the molecule.

The new AdNDP 2.0 code is available free of charge and can be downloaded through the Github source (https://zenodo.org/record/____). The "User's Manual" could be found through the following links: http://ion.chem.usu.edu/~boldyrev/, and http://ion.chem.usu.edu/~boldyrev/nikolay.html. The visualization of the calculation results was performed using ChemCraft 1.8 software.

RESULTS AND DISCUSSION

In our study, we conducted an extended AdNDP analysis of the excited state of three different molecules: H_2O, B_5^+, and $C_2H_4^+$. The choice of these systems was made to illustrate the flexibility of the method in the analysis of various cases. Thus, the water molecule was chosen as the simplest case due to its classical bonding pattern and well-studied properties. Since AdNDP is widely used for the analysis of the clusters, we chose a boron cluster B_5^+ to show the way, how AdNDP 2.0 can describe non-classical chemical bonding patterns of the excited electronic state. A $C_2H_4^+$

species was chosen to show the ability of the algorithm to analyze open shell systems. The results of the analysis for each molecule are shown below.

H_2O molecule

The application of the AdNDP method to the water molecule in ground state (C_{2v}, $1a_1^2 2a_1^2 1b_2^2 3a_1^2 1b_1^2$, $^1A_1$) led us to a classical valence bonding pattern with two 2c-2e σ O-H bonds with ON=1.97 |e| and two *s*- and *p*-type lone pairs on the oxygen with occupation numbers 1.98 and 1.97 |e| respectively (Figure 1, A-bottom). To understand the bonding structure after the vertical excitation, we perform an analysis of the excited state of the water molecule (C_{2v}, $1a_1^2 2a_1^2 1b_2^2 3a_1^2 1b_1^1 4a_1^1$, $^1B_1$) at the geometry of the ground electronic state. We noticed that one electron from *p*-type lone pair of the oxygen transfers to a 3c-1e antibonding orbital. The shape of this orbital is similar to the shape of the canonical molecular $4a_1$ orbital (Figure 1. B). By analyzing the phase sign of this 3c-1e bond we can observe a binding region between two hydrogen atoms and an anti-binding region between hydrogen and oxygen atoms. Using this information, one can predict that the O-H bond will lengthen, and the H-O-H angle will decrease upon the subsequent transformation of the molecular geometry. By performing the optimization of water geometry in the first excited state (the second root of the CASSCF calculations was considered), we can check that our predictions were correct. Indeed, the O-H bonds lengthened from 0.967 Å to 1.066 Å and the H-O-H angle decreased from 104.17˚ to 103.03˚ (Figure 1, A top, B top).

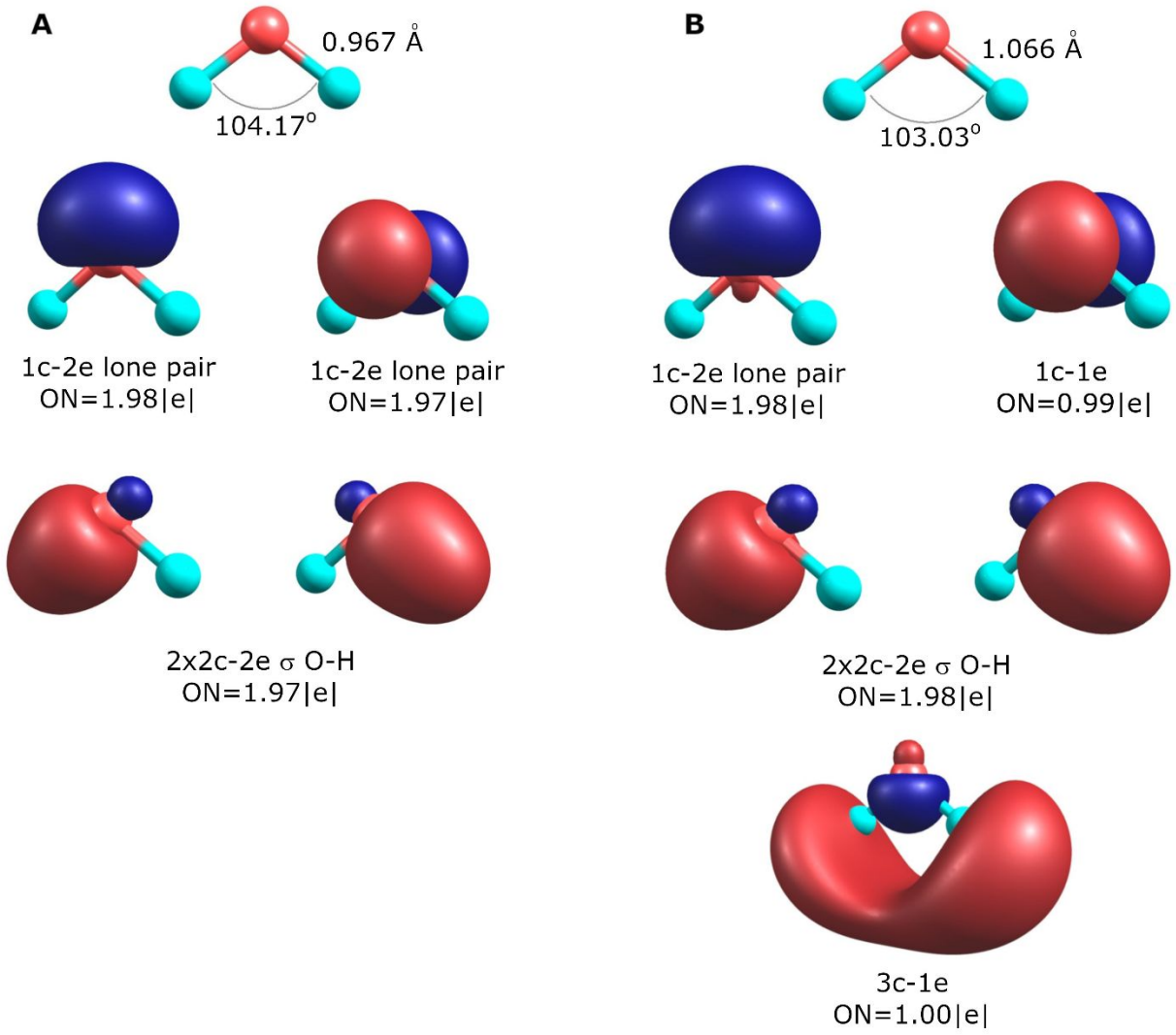

Figure 1. Optimized structures of the water molecule in the ground electronic state (A top) and in the first excited electronic state (B top); the results of the extended AdNDP analysis of the ground state (A bottom) and the first excited state (B bottom) at the ground state optimized geometry.

B_5^+ cluster

According to previous computational works [63], the global minimum structure of B_5^+ cluster belongs to C_{2v} symmetry group and has slightly distorted from the regular pentagon geometry (Figure 2, A-top). The main electronic configuration of the ground state at CASSCF/def2tzvp level

of theory is $1a_1^2 2a_1^2 1b_2^2 3a_1^2 2b_2^2 4a_1^2 3b_2^2 5a_1^2 6a_1^2 4b_2^2 1b_1^2 7a_1^2$, $^1A_1$. The application of the AdNDP method to the valence MOs of ground electronic state of B_5^+ led us to five peripheral 2c-2e σ B-B bonds with ON=1.99-1.96 |e|. Additionally, we found two delocalized 5c-2e bonds with ON=1.92 and 1.88 |e| that are responsible for the σ and π-aromaticity of the system. According to the extended AdNDP analysis of the valence MOs of the B_5^+ cluster in the first excited state ($C_{2v,}$ $1a_1^2 2a_1^2 1b_2^2 3a_1^2 2b_2^2 4a_1^2 3b_2^2 5a_1^2 6a_1^2 4b_2^2 1b_1^2 7a_1^1 1a_2^1$, $^1A_2$), the molecule preserves five peripheral 2c-2e σ B-B bonds with ON=1.95-1.91 |e| and delocalized 5c-2e π bond with ON=1.92 |e|. However, one electron from 5c-2e σ-bond transfers to an excited 5c-1e π*-bond. By analyzing this bonding pattern, one can expect that distances between B1-B2 and B3-B4 will increase. Moreover, the distance B1-B2 will increase more than the distance B3-B4 due to the greater electron density on atoms 1B and 2B. In contrast, distances B1-B3, B2-B4 will not change. Indeed, after the geometry optimization of the excited state using the second root of the CASSCF calculations, one could see that B1-B2 and B3-B4 distances increase from 2.778 Å to 2.854 Å and from 1.553 Å to 1.621 Å, respectively. Also, 1B-3B and 2B-4B distances remain almost unchanged ($\Delta_{(1B-2B)}$ = 0.076 Å, $\Delta_{(3B-4B)}$ = 0.068 Å; $\Delta_{(1B-3B)} = \Delta_{(2B-4B)}$ = -0.009 Å).

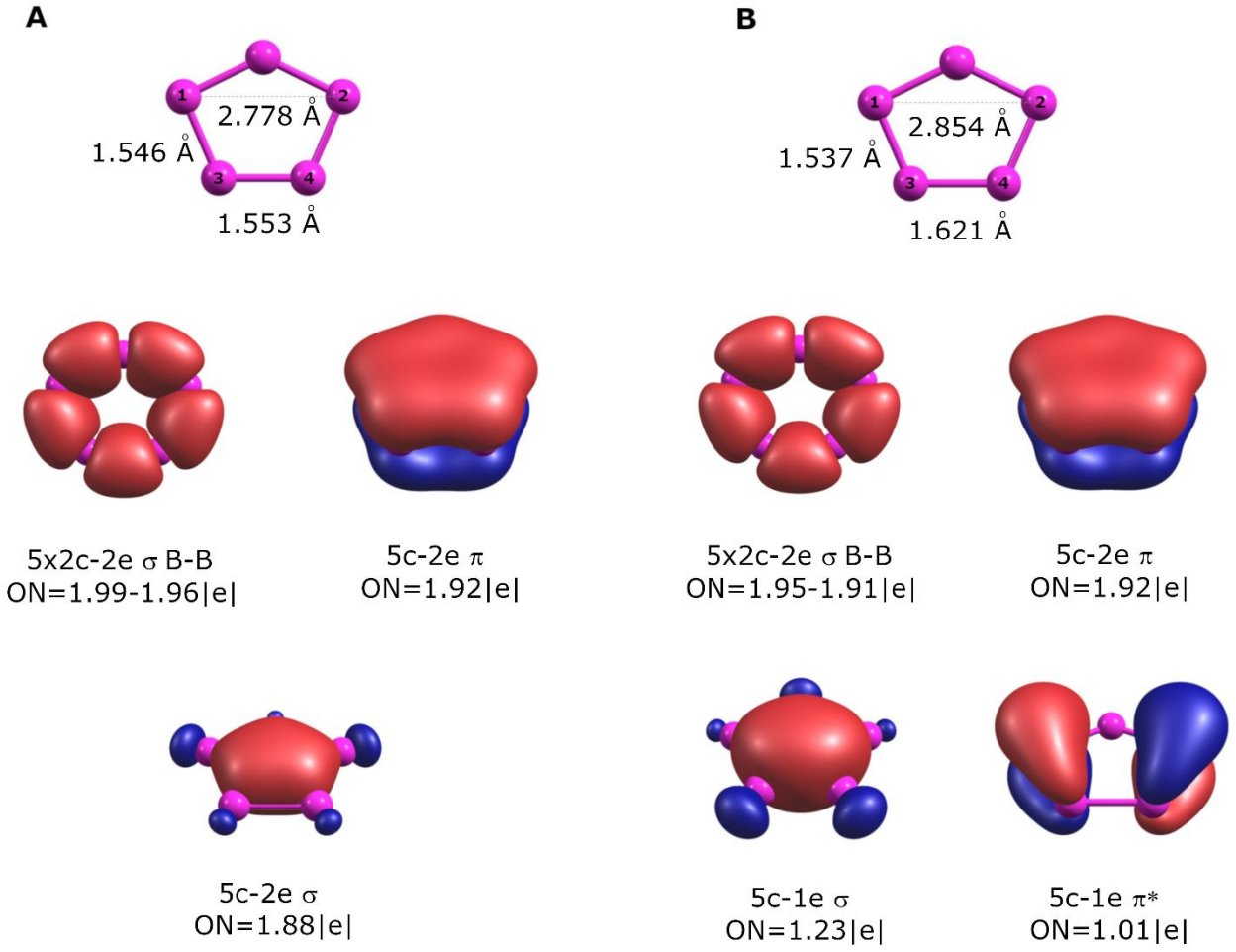

Figure 2. Optimized structures of the B_5^+ cluster in the ground electronic state (A top) and in the first excited electronic state (B top); the results of the extended AdNDP analysis of the ground state (A bottom) and the first excited state (B bottom) at the ground state optimized geometry.

$C_2H_4^+$ species

It has been shown that the ground state geometry of the $C_2H_4^+$ species is not planar and exhibits twisted geometry with the dihedral angle H-C-C-H about 20˚ (D_2 symmetry) [64, 65]. However, spectral data obtained by Willitsch *et al.* suggested that the molecular symmetry may be regarded as D_{2h} rather than D_2 [66]. We conduct an optimization of a twisted and planar geometries at

CCSD(T)/cc-pvqz level of theory. We found that the planar geometry is the first order stationary point with one imaginary frequency and has the total electronic energy higher than the twisted structure by 0.23 kcal/mol. With the inclusion of ZPE corrections, the planar geometry became lower by energy than the twisted isomer (ΔE=-0.01 kcal/mol). Thus, the average vibrational structure has D_{2h} symmetry. Here and below we will investigate bonding structure only for the planar isomer of $C_2H_5^+$ since it is irrelevant in terms of chemical bonding.

Optimized ground state geometry of $C_2H_4^+$ obtained at CASSCF(7,9)/cc-pvdz level of theory is slightly distorted from D_{2h} symmetry (Fig.3 A top). However, for the convenience, we supposed that the structure belongs to D_{2h} symmetry. The ground state has the $1a_g^2 1b_u^2 2a_g^2 2b_u^2 3b_u^2$ $3a_g^2 4a_g^2 1a_u^1$ main electron configuration and the ^2A_u electronic term. Due to the vertical excitation, one electron transfers from $4a_g^2$ orbital to $1a_u^1$ orbital. So the main electron configuration of the first excited state in the geometry of the ground state is $1a_g^2 1b_u^2 2a_g^2 2b_u^2 3b_u^2 3a_g^2 4a_g^1 1a_u^2$ with the term ^2A_g. The AdNDP analysis of the ground state electron configuration shows a classical bonding pattern (Fig.3 A bottom) with four 2c-2e σ C-H bonds (ON=1.99-1.97 |e|), one 2c-2e σ C-C bond (ON = 1.97 |e|) and one electron sitting on 2c-1e π C-C bond (ON = 0.99 |e|).

Intriguing results were obtained from the AdNDP analysis of the first excited state (Fig. 3 B bottom). We found, that due to the vertical excitation, the occupation number of the 2c-2e π C-C bond increases by 0.9 |e|. This fact indicates that a classical C-C double bond exists in the excited structure. Thus, one can expect a decrease of the C-C distance since the bonding interaction between two atoms increases. Indeed, we observed such geometry transformation optimizing geometry in the excited state ($\Delta_{(C-C)}$ = -0.176 Å). Because of the high symmetry of the molecule, the electron transfers from two σ C-H bonds (0.5 |e| from each bond). Therefore, it is possible to predict a further increase of the C-H distance ($\Delta_{(C-H)}$= 0.101 Å).

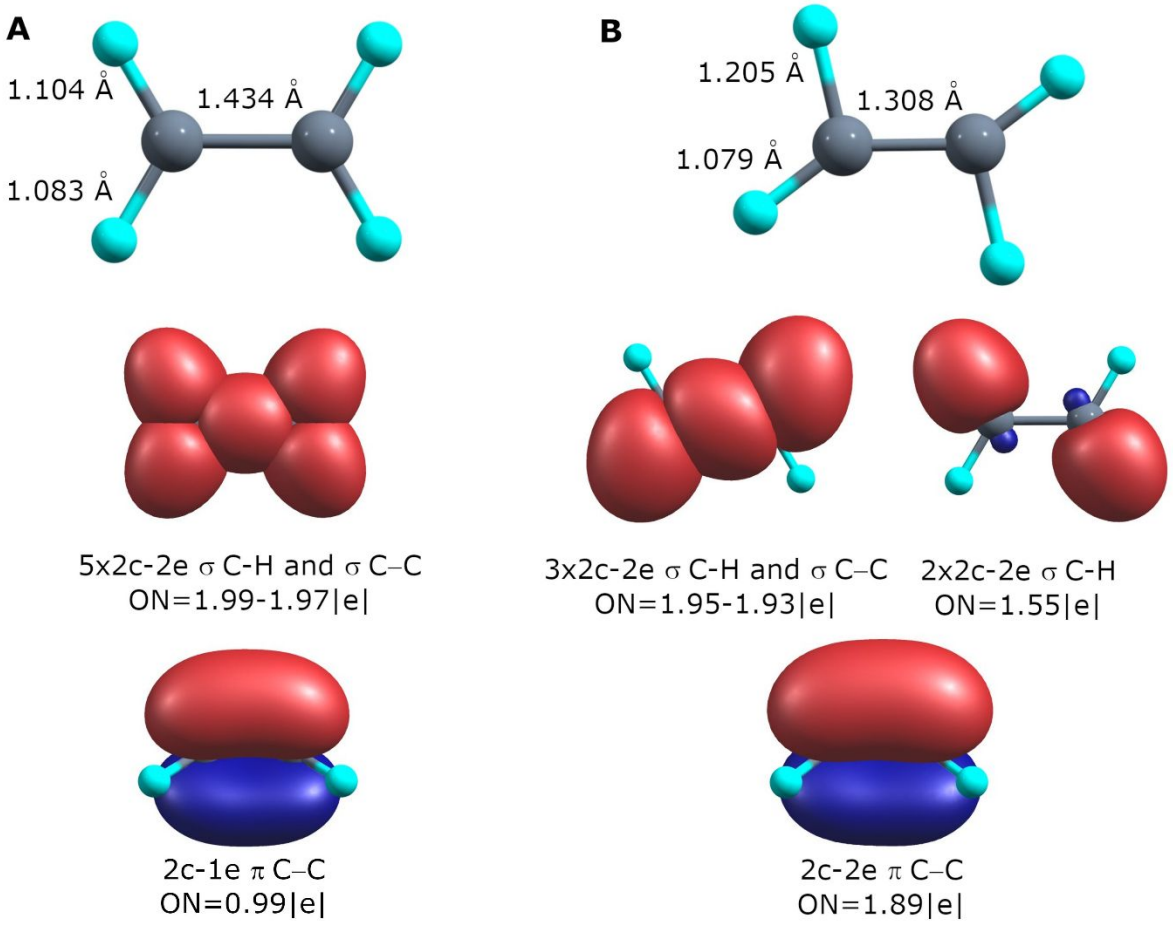

Figure 3. Optimized structures of the $C_2H_4^+$ molecule in the ground electronic state (A top) and in the first excited electronic state (B top); the results of the extended AdNDP analysis of the ground state (A bottom) and the first excited state (B bottom) at the ground state optimized geometry.

CONCLUSIONS

An updated AdNDP 2.0 algorithm was introduced. New features of the algorithm such as distance restrictions, symmetric direct search, analysis of open shell systems, and excited states bonding analysis greatly expand the applicability of the method. We showed that the chemical bonding patterns of the excited state molecules, obtained by an updated AdNDP 2.0 code, are

comprehensive and consistent with the chemical intuition. Moreover, by analyzing a bonding pattern of the excited state molecule in the geometry of the ground state, one can easily predict the subsequent geometry transformation upon an electronic excitation. We hope that our new AdNDP method will become a useful tool in photochemistry, photoelectron spectroscopy, electron spectroscopy, and other areas of chemistry where excited states are involved.

CONFLICTS OF INTEREST

There are no conflicts to declare.

ACKNOWLEDGMENTS

The work was supported by the USA National Science Foundation (Grant CHE-1664379) to A.I.B. Also, authors are grateful for the discussion and their comments about new AdNDP 2.0 code to Dmitry Zubarev, Maksim Kulichenko, Katie Lundell and Nikita Fedik.

REFERENCES

[1] G. N. Lewis, *J. Am. Chem. Soc.*, 1916, **38**, 762.

[2] F. Hund, *Z. Phys.*, 1931, **73**, 1.

[3] R. S. Mulliken, *Phys. Rev.*, 1932, **41**, 49.

[4] L. Pauling, *J. Am. Chem. Soc.*, 1931, **53**, 1367.

[5] L. Pauling, *J. Am. Chem. Soc.*, 1931, **53**, 3225.

[6] W. Heitler and F. London, *Z. Phys.*, 1927, **44**, 455.

[7] J. C. Slater, *Phys. Rev.*, 1931, **37**, 481.

[8] J. C. Slater, *Phys. Rev.*, 1931, **38**, 1109.

[9] R. F. W. Bader, *Atoms in Molecules: A Quantum Theory*, Oxford University Press, Oxford, 1990.

[10] V. K. Artman, *Z. Naturforsch.*, 1946, **1**, 426.

[11] J. E. Lenard-Jones, *Proc. R. Soc. London, Ser. A*, 1949, **198**, 14.

[12] J. E. Lenard-Jones, *Proc. R. Soc. London, Ser. A*, 1949, **198**, 1.

[13] R. Daudel, *Quantum Theory of the Chemical Bond*, Reidel, Dordrecht, 1974.

[14] R. F. W. Bader and M. E. Stephens, *J. Am. Chem. Soc.*, 1975, **97**, 7391.

[15] W. L. Luken and J. C. Culberson, *Int. J. Quantum Chem.*, 1982, **22**, 265.

[16] A. D. Becke and K. E. Edgecombe, *J. Chem. Phys.*, 1990, **92**, 5397.

[17] B. Silvi and A. Savin, *Nature*, 1994, **371**, 683.

[18] P. A Fuentealba, *Int. J. Quantum Chem.*, 1998, **69**, 559.

[19] R. Ponec and D. L. Cooper, *J. Phys. Chem. A*, 2007, **111**, 11294.

[20] F. Fantuzzi and M. A. C. Nascimento, *J. Chem. Theory Comput.*, 2014, **10**, 2322.

[21] J. H. Lange and I. Cukrowski, *J. Comput. Chem.*, 2018, **39**, 1517.

[22] B. G. Janesko, G. Scalmani and M. J. Frisch, *J. Chem. Phys.*, 2014, **141**, 144104.

[23] E. Ramos-Cordoba, P. Salvador and M. Reiher, *Chem. Eur. J.*, 2013, **19**, 15267.

[24] D. L. Cooper, R. Ponec and M. Kohout, *Mol. Phys.*, 2016, **114**, 1270.

[25] K. B. Wiberg, *Tetrahedron*, 1968, **24**, 1083.

[26] I. Mayer, *Chem. Phys. Lett.*, 1983**, 97**, 270.

[27] I. Mayer, *Int. J. Quantum Chem.*, 1986, **29**, 73.

[28] M. Giambiagi, M. S. Giambiagi and K. C. Mundim, *Struct. Chem.*, 1990, **1**, 423.

[29] A. B. Sannigrahi and T. Kar, *Chem. Phys. Lett.*, 1990, **173**, 569.

[30] F. Feixas, M. Sola, J. M. Barroso, J. M. Ugalde and E. Matito, *J. Chem. Theory Comput.*, 2014, **10**, 3055.

[31] R. L. Fulton, *J. Phys. Chem.*, 1993, **97**, 7516.

[32] R. L. Fulton and S. T. Mixon, *J. Phys. Chem.*, 1993, **97**, 7530.

[33] X. Fradera, M. A. Austen and R. F. W. Bader, *J. Phys. Chem. A*, 1999, **103**, 304.

[34] I. Mayer, *J. Quantum Chem.*, 1984, **26**, 151.

[35] I. Mayer, *J. Quantum Chem.*, 1985, **28**, 419.

[36] I. Mayer, *J. Quantum Chem.*, 1986, **29**, 477.

[37] E. Matito, M. Sola, P. Salvador and M. Duran, *Faraday Discuss.*, 2007, **135**, 325.

[38] J. M. Foster and S. F. Boys, *Rev. Mod. Phys.*, 1960, **32**, 300.

[39] C. Edmiston and K. Ruedenberg, *Rev. Mod. Phys.*, 1963, **35**, 457.

[40] J. Pipek and P. G. Mezey, *J. Chem. Phys.*, 1989, **90**, 4916.

[41] J. P. Foster and F. Weinhold, *J. Am. Chem. Soc.*, 1980, **102**, 7211.

[42] A. E. Reed, L. A. Curtiss and F. Weinhold, *Chem. Rev.*, 1988, **88**, 899.

[43] F. Weinhold and C. R. Landis, *Valency and Bonding: A Natural Bond Orbital Donor–Acceptor Perspective*, Cambridge University Press, Cambridge, UK, 2005.

[44] L. Gonzalez, D. Escudero and L. Serrano-Andres, *ChemPhysChem*, 2012, **13**, 28.

[45] E. S. Kadantsev and H. L. Schmider, *Int. J. Quantum Chem.*, 2008, **108**, 1.

[46] T. Burnus, M. A. L. Marques and E. K. U. Gross, *Phys. Rev. A*, 2005, **71**, 010501.

[47] J. Cullen, M. Krykunov and T. Ziegler, *Chem. Phys.*, 2011, **391**, 11.

[48] T. Ziegler, M. Krykunov and J. Cullen, *J. Chem. Phys.*, 2012, **136**, 124107.

[49] M. A. Blanco, A. Martin Pendas and E. Francisco, *J. Chem. Theory Comput.*, 2005, **1**, 1096.

[50] J. Jara-Cortés, J. M. Guevara-Vela, A. M. Pendás and J. Hernández-Trujillo, *J. Comput. Chem.*, 2017, **38**, 957.

[51] F. Feixas, E. Matito, J. Poater and M. Solà, *Chem. Soc. Rev.*, 2015, **44**, 6434.

[52] L. Gutiérrez-Arzaluz, F. Cortés-Guzmán, T. Rocha-Rinza and J. Peón, *Phys. Chem. Chem. Phys.*, 2015, **17**, 31608.

[53] M. Estévez-Fregosoa and J. Hernández-Trujillo, *Phys. Chem. Chem. Phys.*, 2016, **18**, 11792.

[54] L. Vannay, E. Bremond, P. Silva and C. Corminboeuf, *Chem. Eur. J.*, 2016, **22**, 18442.

[55] D. Y. Zubarev and A. I. Boldyrev, *J. Org. Chem.*, 2008, **73**, 9251.

[56] D. Y. Zubarev and A. I. Boldyrev, *Phys. Chem. Chem. Phys.*, 2008, **10**, 5207.

[57] P. J. Knowles and H.-J. Werner, *Chem. Phys. Lett.*, 1985, **115**, 259.

[58] T. H. Dunning, *J. Chem. Phys.*, 1989, **90**, 1007.

[59] K. Raghavachari, J. S. Binkley, R. Seeger and J. A. Pople, *J. Chem. Phys.*, 1980, **72**, 650.

[60] F. Weigend and R. Ahlrichs, *Phys. Chem. Chem. Phys.*, 2005, **7**, 3297.

[61] K. Raghavachari, G. W. Trucks, J. A. People and M. Head-Gordon, *Chem. Phys. Lett.*, 1989, **157**, 479.

[62] J. D. Watts, J. Gauss and R. J. Bartlett, *J. Chem. Phys.*, 1993, **98**, 8718.

[63] A. N. Alexandrova, A. I. Boldyrev, H.-J. Zhai and L.-S. Wang, *Coord. Chem. Rev.*, 2006, **250**, 2811.

[64] B. Joalland, T. Mori, T. J. Martinez and A. G. Suits, *J. Phys. Chem. Lett.*, 2014, **5**, 1467.

[65] M. L. Abrams, E. F. Valeev and C. D. Sherrill, *J. Phys. Chem. A*, 2002, **106**, 2671.

[66] S. Willitsch, U. Hollenstein and F. Merkt, *J. Chem. Phys.*, 2004, **120**, 1761.

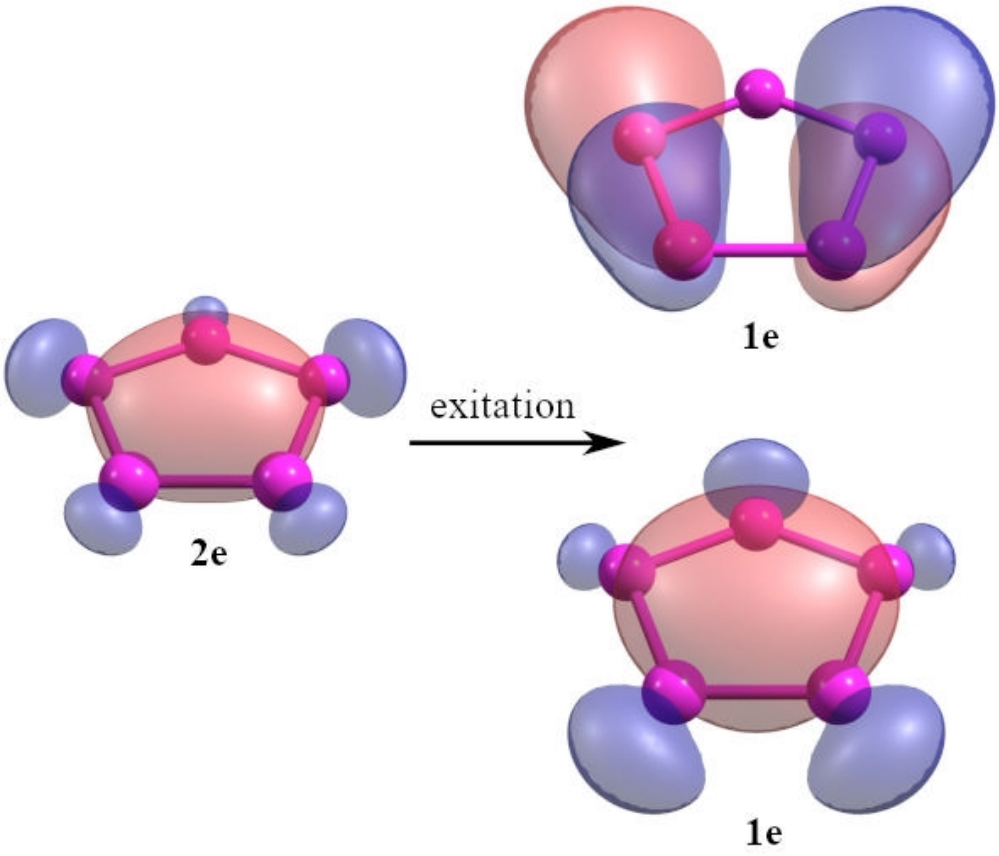

50x50mm (300 x 300 DPI)